Spin-Transfer-Driven Ferromagnetic Resonance of Individual Nanomagnets

J. C. Sankey, P. M. Braganca, A. G. F. Garcia, I. N. Krivorotov, R. A. Buhrman, and D. C. Ralph
Cornell University, Ithaca, New York 14853, USA
(Received 4 February 2006; published 5 June 2006)

We demonstrate a technique that enables ferromagnetic resonance measurements of the normal modes for magnetic excitations in individual nanoscale ferromagnets, smaller in volume by more than a factor of 50 compared to individual ferromagnetic samples measured by other resonance techniques. Studies of the resonance frequencies, amplitudes, linewidths, and line shapes as a function of microwave power, dc current, and magnetic field provide detailed new information about the exchange, damping, and spin-transfer torques that govern the dynamics in magnetic nanostructures.

DOI: 10.1103/PhysRevLett.96.227601 PACS numbers: 76.50.+g, 72.25.Ba, 75.30.Ds, 75.75.+a

Ferromagnetic resonance (FMR) is the primary technique for learning about the forces that determine the dynamical properties of magnetic materials. However, conventional FMR detection methods lack the sensitivity to measure individual sub-100-nm-scale devices that are of interest for fundamental physics studies and for a broad range of memory and signal-processing applications. For this reason, many new techniques are being investigated for probing magnetic dynamics on small scales, including Brillouin scattering [1] and FMR detected by Kerr microscopy [2], scanning probes [3,4], x rays [5], and electrical techniques [6]. Here we demonstrate a simple new form of FMR that uses innovative methods to both drive and detect magnetic precession, thereby enabling FMR studies for the first time on individual sub-100-nm devices and providing a detailed new understanding of their magnetic modes. We excite precession not by applying an ac magnetic field as is done in other forms of FMR, but by using the spin-transfer torque from a spin-polarized ac current [7,8]. We detect the resulting magnetic motions electrically. We demonstrate detailed studies of FMR in single nanomagnets as small as $30 \times 90 \times 5.5$ nm^3, and the method should be scalable to investigate much smaller samples as well. Our technique is similar to methods developed independently by Tulapurkar *et al.* [9] for radio-frequency detection, but we will demonstrate that the peak shapes measured there were likely not simple FMR.

We have achieved the following new results: (i) We measure magnetic normal modes of a single nanomagnet, including both the lowest-frequency fundamental mode and higher-order spatially nonuniform modes. (ii) By comparing the FMR spectrum to signals excited by a dc spin-polarized current, we demonstrate that different dc biases can drive different normal modes. (iii) From the resonance line shapes, we distinguish simple FMR from a regime of phase locking. (iv) From the resonance linewidths, we achieve efficient measurements of magnetic damping in a single nanomagnet.

Our samples have a nanopillar structure [Fig. 1(a), inset], consisting of two magnetic layers—20 nm of permalloy (Py = $Ni_{81}Fe_{19}$) and 5.5 nm of a $Py_{65}Cu_{35}$ alloy—separated by a 12 nm copper spacer (see details in [10]). We pattern the layers to have approximately elliptical cross sections using ion milling. We focus here on one 30×90 nm^2 device, but we also obtained similar results in 40×120 nm^2 and 100×200 nm^2 samples. We use different materials for the two magnetic layers so that by applying a perpendicular magnetic field H we can induce an offset angle between their equilibrium moment directions (both the spin-transfer torque and the small-angle resistance

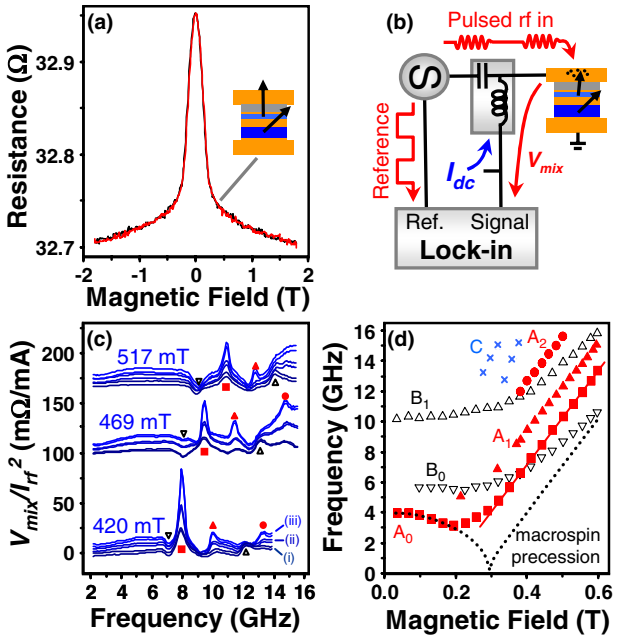

FIG. 1 (color online). (a) Room-temperature magnetoresistance as a function of field perpendicular to the sample plane. Inset: Cross-sectional sample schematic, with arrows denoting a typical equilibrium moment configuration in a perpendicular field. (b) Schematic of circuit used for FMR measurements. (c) FMR spectra measured at several values of magnetic field, at I_{dc} values (i) 0, (ii) 150 μA, and (iii) 300 μA, offset vertically. Symbols identify the magnetic modes plotted in (d). Here $I_{rf} = 300$ μA at 5 GHz and decreases by ~50% as f increases to 15 GHz [10]. (d) Field dependence of the modes in the FMR spectra. The solid line is a linear fit, and the dotted line would be the frequency of completely uniform precession.

response are zero otherwise). The room-temperature magnetoresistance [Fig. 1(a)] shows that the PyCu moment saturates out of plane at $\mu_0 H \approx 0.3$ T, while the larger moment of Py does not saturate until approximately $\mu_0 H > 1$ T [11]. All of our FMR measurements are performed at low temperature ($\leq$10 K), and the direction of H is approximately perpendicular to the layers ($\hat{z}$ direction), tilted $\sim 5°$ along the long axis of the ellipse ($\hat{x}$ direction) to control in-plane moment components. Positive currents correspond to electron flow from the PyCu to the Py layer. Using a bias tee, we apply current at both microwave frequencies ($I_{\rm rf}\cos 2\pi f t$) and dc ($I_{\rm dc}$) while measuring the dc voltage across the sample $V_{\rm dc}$ [Fig. 1(b)]. If the frequency f is set near a resonance of either magnetic layer, the layer will precess, producing a time-dependent resistance:

$$R(t) = R_0 + \Delta R(t) = R_0 + \mathrm{Re}\left(\sum_{n=0}^{\infty} \Delta R_{nf} e^{in2\pi f t}\right), \quad (1)$$

where ΔR_{nf} can be complex. The voltage $V(t) = I(t)R(t)$ will contain a term involving mixing between $I_{\rm rf}$ and $\Delta R(t)$, so that the measured dc voltage will be

$$V_{\rm dc} = I_{\rm dc}(R_0 + \Delta R_0) + \frac{1}{2} I_{\rm rf} |\Delta R_f| \cos(\delta_f), \quad (2)$$

where δ_f is the phase of ΔR_f. The final term enables measurement of spin-transfer-driven FMR. To reduce background signals and noise, we chop the microwave current bias at 1.5 kHz and measure the dc mixing signal $V_{\rm mix} = V_{\rm dc} - I_{\rm dc} R_0$ using a lock-in amplifier.

In Fig. 1(c) we plot the FMR response $V_{\rm mix}/I_{\rm rf}^2$ measured for $I_{\rm dc}$ near 0. We observe several resonances, appearing as either peaks or dips in $V_{\rm mix}$. An applied $I_{\rm dc}$ can decrease the width of some resonances and make them easier to discern, as discussed below. By studying the field dependence of the largest resonances [Fig. 1(d)], we identify two groups that we will call normal modes A_0, A_1, A_2 (solid symbols) and B_0, B_1 (open symbols). Above $\mu_0 H = 0.3$ T, the field required to saturate the PyCu moment along $\hat{z}$, the frequencies of A_0, A_1, and A_2 shift linearly in parallel with slope $df/dH = g\mu_B\mu_0/h$, where $g = 2.2 \pm 0.1$. As expected for the modes of a thin-film nanomagnet [13], the measured frequencies are shifted above that of uniform precession of a bulk film, $f_{\rm film} = (g\mu_B/h)[\mu_0 H - \mu_0 M_{\rm eff}]$, with $\mu_0 M_{\rm eff} = 0.3$ T. This H dependence provides initial evidence that A_0, A_1, and A_2 are magnetic modes of the PyCu layer (additional evidence is presented later). The other two large resonances, B_0 and B_1, also shift together, with a weaker dependence on H. This is the behavior expected for modes of the Py layer, because the values of H shown in Fig. 1(d) are not large enough to saturate the Py layer out of plane. To avoid coupling between modes in different layers, we perform our detailed measurements at fields where the mode frequencies are well separated. In addition to these modes, we observe small signals [not shown in Fig. 1(d)] at twice the frequencies of the main modes and near frequency sums (modes C).

Based on comparisons to simulations [13,14] and that the lowest-frequency resonances produce the largest resistance signals, we propose that A_0 and B_0 correspond to the lowest-frequency normal mode of the PyCu and Py layer, respectively. This mode should have the most spatially uniform precession amplitude (albeit not exactly uniform) [13,14]. The higher-frequency resonances A_1, A_2, and B_1 must correspond to higher-order nonuniform modes. The observed frequencies and frequency intervals are in the range predicted for normal modes of similarly shaped nanoscale samples [13,14].

Next we compare the FMR measurements to spontaneous precessional signals that can be excited by $I_{\rm dc}$ alone ($I_{\rm rf} = 0$) [15,16]. The power spectral density of resistance oscillations for dc-driven excitations at 420 mT is shown in Fig. 2(a). We examine $I_{\rm dc} > 0$, which gives the sign of torque to drive excitations in the PyCu layer only [12]. A single peak appears in the dc-driven spectral density above a critical current $I_c = 0.3$ mA, and moves to higher frequency with increasing $I_{\rm dc}$. The increase in frequency can be identified with an increasing precession angle, which decreases the average demagnetizing field along $\hat{z}$ [12]. At larger $I_{\rm dc}$, we observe additional peaks at higher f and switching of the precession frequency between different values, similar to the results of previous measurements [12,15,16] that have not been well explained before.

The FMR signals are displayed in Fig. 2(b) at the same values of $I_{\rm dc}$ shown in Fig. 2(a). We find that the FMR fundamental mode A_0 that we identified above with the PyCu layer is the mode that is excited at the threshold for dc-driven excitations. When $I_{\rm dc}$ is large enough that the dc-driven mode begins to increase in frequency (585 μA), the shape of this FMR changes from a simple Lorentzian to a more complicated structure with a dip at low frequency and a peak at high frequency. The FMR peaks A_1 and A_2 also

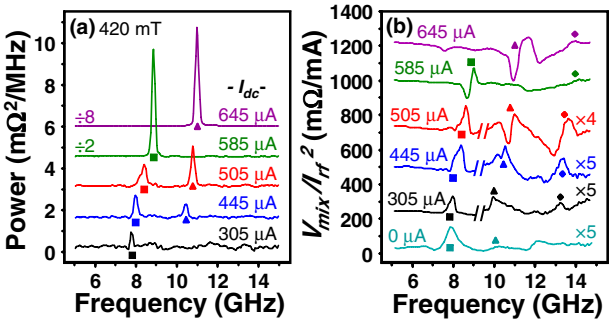

FIG. 2 (color online). Comparison of FMR spectra to dc-driven precessional modes. (a) Spectral density of dc-driven resistance oscillations for different values of $I_{\rm dc}$ (labeled), with $\mu_0 H = 370$ mT and $I_{\rm rf} = 0$. (b) FMR spectra at the same values of $I_{\rm dc}$, measured with $I_{\rm rf} = 270$ μA at 10 GHz. The high-f portions of the 305 μA, 445 μA, and 505 μA traces are amplified to better show small resonances. The $I_{\rm dc} = 0$ curve is the same as in Fig. 1(c).

vary strongly in peak shape and frequency as a function of positive I_{dc}, in a manner similar to A_0, confirming that A_1 and A_2 (like A_0) are associated with the PyCu layer. The FMR modes B_0 and B_1 that we identified with the Py layer do not shift significantly in f as a function of positive I_{dc}. This is expected, because positive I_{dc} is the wrong sign to excite spin-transfer dynamics in the Py layer [7].

There has been significant debate about whether the magnetic modes which contribute to the dc-spin-transfer-driven precessional signals correspond to approximately uniform macrospin precession or to nonuniform spin-wave instabilities [17–20]. Our FMR measurements show directly that, at I_c, the dc-driven peak frequency is equal to that of the lowest-frequency rf-driven mode, the one expected to be most spatially uniform [13]. Higher values of I_{dc} can also excite the spatially nonuniform mode A_1 and even produce mode hopping so that mode A_1 can be excited when mode A_0 is not.

In order to analyze the FMR peak shapes, we make the simplifying assumption that the lowest-frequency modes A_0 and B_0 can be approximated by a macrospin model, with the Slonczewski form of the spin-transfer torque [7]. The small-amplitude resonance is predicted [10] to have a simple Lorentzian line shape,

$$V_{\mathrm{mix}}(f) \propto \frac{I_{\mathrm{rf}}^2/\Delta_0}{1+[(f-f_0)/\Delta_0]^2}. \qquad (3)$$

Here f_0 is the unforced precession frequency. The width Δ_0 predicted for the PyCu layer in our experimental geometry is, to within 1% error for $\mu_0 H > 0.5$ T [10],

$$\Delta_0 = \alpha f_0, \qquad (4)$$

where α is the Gilbert damping parameter. As predicted by Eq. (3), we find that the measured FMR peak for mode A_0 at $I_{dc} = 0$, for sufficiently small values of I_{rf}, is fit accurately by a Lorentzian, the amplitude scales $V_{\mathrm{mix}} \propto I_{\mathrm{rf}}^2$, and the width is independent of I_{rf}, [Figs. 3(a) and 4(a)]. Our minimum measurable precession angle is $\approx 0.2°$. For $I_{rf} > 0.35$ mA, the peak eventually shifts to higher frequency and the shape becomes asymmetric, familiar properties for nonlinear oscillators [21]. From the magnitude of the frequency shift in similar signals [Fig. 3(b), inset], we estimate that the largest precession angle we have achieved is approximately 40°.

The peak shape for mode B_0 is also to good accuracy Lorentzian for small I_{dc}, but with negative sign. This sign is expected because when the Py moment precesses in resonance, the positive current pushes the Py moment angle closer to the PyCu moment, giving a negative resistance response. The FMR peak shapes for the higher-order modes A_1, A_2, and B_1 are not as well fit by Lorentzians. We plot the spectrum of dc-driven excitations for $I_{dc} = 0.52$ mA, $I_{rf} = 0$ in Fig. 3(b). The width is much narrower than the FMR spectrum for the same mode (inset), confirming arguments that the linewidths in these two types of measurements are determined by different physics [22].

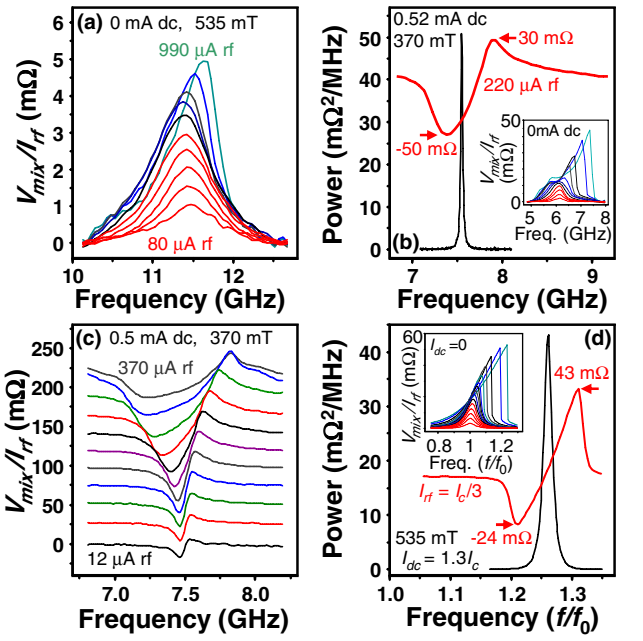

FIG. 3 (color online). (a) FMR peak shape for mode A_0 at $I_{dc} = 0$ and different values of I_{rf}: from bottom to top, traces 1–5 span $I_{rf} = 80$–340 μA in equal increments, and traces 5–10 span 340–990 μA in equal increments. (b) Bottom curve: spectral density of dc-driven resistance oscillations for mode A_0, showing a peak with a half width at half maximum = 13 MHz. Top curve: FMR signal at the same bias conditions, showing the phase-locking peak shape. Inset: Evolution of the FMR peak for mode A_0 at 370 mT, $I_{dc} = 0$, for I_{rf} from 30 μA to 1160 μA. (c) Evolution of the FMR signal for mode A_0 in the phase-locking regime at $I_{dc} = 0.5$ mA, $\mu_0 H = 370$ mT, for (bottom to top) I_{rf} from 12 to 370 μA, equally spaced on a logarithmic scale. (d) Results of macrospin simulations for the dc-driven dynamics and the FMR signal [10].

We noted above that the FMR peak shape changes from a Lorentzian to a more complex shape for sufficiently large values of I_{dc}. [See the detailed resonance shapes in Figs. 3(b) and 3(c).] This shape change can be explained as a consequence of phase locking between I_{rf} and the large-amplitude precession excited by I_{dc} [23–26]. When the precession frequency increases with precession amplitude, the rf current can force the amplitude on the low-f side of the resonance to be smaller than the equilibrium dc-driven trajectory. Under these conditions, the precession phase locks approximately out of phase with the applied rf current ($\delta_f \approx 180°$), giving negative values of V_{mix}. Frequencies on the high-f side of the resonance produce phase locking approximately in phase with the drive and a positive V_{mix}. We have confirmed this picture by numerical integration of the macrospin model [Fig. 3(d)] [10]. Recently, Tulapurkar *et al.* [9] measured similar peak shapes, and proposed that they were caused by simple FMR with a torque mechanism different from the Slonczewski theory. We suggest instead that the peak shapes in [9] may be due either to phase locking with thermally excited precession at room temperature (rather

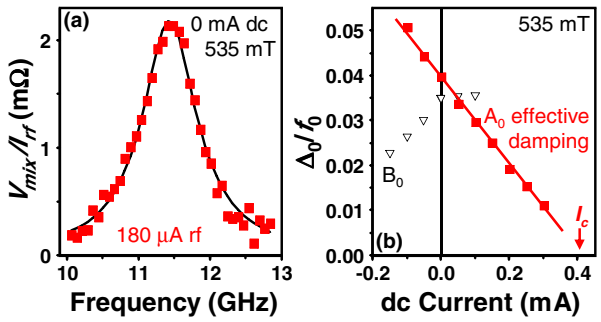

FIG. 4 (color online). (a) Detail of the peak shape for mode A_0, at $I_{dc} = 0$, $I_{rf} = 180$ μA, $\mu_0 H = 535$ mT, with a fit to a Lorentzian line shape. (b) Dependence of linewidth on I_{dc} for modes A_0 and B_0, for $\mu_0 H = 535$ mT. For the PyCu layer mode A_0, Δ_0/f_0 is equal to the magnetic damping α. The critical current is $I_c = 0.40 \pm 0.03$ mA at $\mu_0 H = 535$ mT, as measured independently by the onset of dc-driven resistance oscillations.

than simple FMR), or to the superposition of two FMR signals from different layers (one positive signal like that of A_0 and one negative like B_0).

A benefit of measuring the Lorentzian line shape of simple FMR is that the linewidth allows a measurement of the magnetic damping α, using Eq. (4). It is highly desirable to minimize the damping in spin-transfer-driven memory devices so as to decrease the current needed for switching [7]. Previously, α in magnetic nanostructures could only be estimated by indirect means [27,28]. As shown in Fig. 4(b), for $I_{dc} = 0$ we measure $\alpha = 0.040 \pm 0.001$ for the PyCu layer. This is larger than the damping for $Py_{65}Cu_{35}$ films in identically prepared large-area multilayers as measured by conventional FMR, $\alpha_{film} = 0.021 \pm 0.003$. The cause of the extra damping in our nanopillars is not known, but it may be due to coupling with an antiferromagnetic oxide along the sides of the device [29]. As a function of increasing I_{dc}, the theory of spin-transfer torques predicts that the effective damping should decrease linearly, going to zero at the threshold for the excitation of dc-driven precession [7]. This is precisely what we find for mode A_0 [Fig. 4(b)]. In contrast, the linewidth of mode B_0 decreases with decreasing I_{dc}. This is as expected for a Py-layer mode, because the sign of the spin-transfer torque should promote dc-driven precession in the Py layer at negative I_{dc}.

We have demonstrated that spin-transfer-driven FMR measurements provide detailed information about the dynamics of both the fundamental and higher-order magnetic normal modes in single sub-100-nm-scale magnetic samples, in both linear and nonlinear regimes. We achieve direct measurements of damping in single nanostructures, show how the damping is tunable by I_{dc}, and determine which modes are excited by large dc spin-transfer torques. Spin-transfer-driven FMR will be of immediate utility in understanding and optimizing magnetic dynamics in nanostructures used for memory and microwave signal-processing applications. Furthermore, both spin-transfer torques and magnetoresistance measurements become increasingly effective on smaller size scales. The same technique may therefore enable new fundamental studies of even smaller magnetic samples, approaching the molecular limit.

We thank J.-M. L. Beaujour, A. D. Kent, and R. D. McMichael for performing FMR measurements on our bulk multilayers. We acknowledge support from the Army Research Office and from the NSF/NSEC program through the Cornell Center for Nanoscale Systems. We also acknowledge NSF support through use of the Cornell Nanofabrication Facility/NNIN and the Cornell Center for Materials Research facilities.

[1] S. O. Demokritov and B. Hillebrands, Top. Appl. Phys. **83**, 65 (2002).
[2] S. Tamaru *et al.*, J. Appl. Phys. **91**, 8034 (2002).
[3] M. M. Midzor *et al.*, J. Appl. Phys. **87**, 6493 (2000).
[4] R. Meckenstock *et al.*, Rev. Sci. Instrum. **74**, 789 (2003).
[5] G. Boero *et al.*, Appl. Phys. Lett. **87**, 152503 (2005).
[6] S. E. Russek and S. Kaka, IEEE Trans. Magn. **36**, 2560 (2000).
[7] J. C. Slonczewski, J. Magn. Magn. Mater. **159**, L1 (1996).
[8] L. Berger, Phys. Rev. B **54**, 9353 (1996).
[9] A. A. Tulapurkar *et al.*, Nature (London) **438**, 339 (2005).
[10] See EPAPS Document No. E-PRLTAO-96-047623 for more information about circuit calibration and data analysis. For more information on EPAPS, see http://www.aip.org/pubservs/epaps.html.
[11] The 20 nm Py layer used here has a stronger demagnetizing field than the 3 nm layer of Ref. [12].
[12] S. I. Kiselev *et al.*, Phys. Rev. Lett. **93**, 036601 (2004).
[13] R. D. McMichael and M. D. Stiles, J. Appl. Phys. **97**, 10J901 (2005).
[14] B. Montigny and J. Miltat, J. Appl. Phys. **97**, 10C708 (2005).
[15] S. I. Kiselev *et al.*, Nature (London) **425**, 380 (2003).
[16] W. H. Rippard *et al.*, Phys. Rev. Lett. **92**, 027201 (2004).
[17] M. L. Polianski and P. W. Brouwer, Phys. Rev. Lett. **92**, 026602 (2004).
[18] M. D. Stiles, J. Xiao, and A. Zangwill, Phys. Rev. B **69**, 054408 (2004).
[19] B. Özyilmaz *et al.*, Phys. Rev. B **71**, 140403(R) (2005).
[20] A. Brataas, Y. Tserkovnyak, and G. E. W. Bauer, Phys. Rev. B **73**, 014408 (2006).
[21] L. D. Landau and E. M. Lifshitz, *Mechanics* (Pergamon, Oxford, 1976), Sec. 29.
[22] J. C. Sankey *et al.*, Phys. Rev. B **72**, 224427 (2005).
[23] W. H. Rippard *et al.*, Phys. Rev. Lett. **95**, 067203 (2005).
[24] S. Kaka *et al.*, Nature (London) **437**, 389 (2005).
[25] F. B. Mancoff *et al.*, Nature (London) **437**, 393 (2005).
[26] M. Tsoi *et al.*, Nature (London) **406**, 46 (2000).
[27] P. M. Braganca *et al.*, Appl. Phys. Lett. **87**, 112507 (2005).
[28] I. N. Krivorotov *et al.*, Science **307**, 228 (2005).
[29] N. C. Emley *et al.*, cond-mat/0510798.